STUDY OF GAS HYDRATE FORMATION AND DEPOSITION MECHANISMS IN HYDROCARBON SYSTEMS

Erlend O. Straume, erlend.straume@gmail.com
Celina Kakitani, ckakitani@gmail.com
Department of Mechanical and Materials Engineering, Federal University of Technology of Paraná, Av. Sete de Setembro, 3165 - Rebouças CEP 80230-901, Curitiba - PR, Brazil

Daniel Merino-Garcia, dmerinog@repsol.com
Repsol Sinopec Brasil, Praia de Botafogo, 300 / 3º andar, CEP 22250-040, Rio de Janeiro - RJ, Brazil

Rigoberto E.M. Morales, rmorales@utfpr.edu.br
Department of Mechanical and Materials Engineering, Federal University of Technology of Paraná, Av. Sete de Setembro, 3165 - Rebouças CEP 80230-901, Curitiba - PR, Brazil

Amadeu K. Sum, asum@mines.edu
Chemical & Biological Engineering Department, Colorado School of Mines, 1613 Illinois St., Golden, CO 80401, USA

Abstract. *"Hydrate Management" strategies in oil and gas production differ from standard "Hydrate Avoidance" design in the fact that, instead of focusing on preventing hydrate formation, these strategies focus on ensuring flow and avoiding blockage formation in multiphase flow conditions where hydrates are stable. In order to safely implement hydrate management strategies, it is required to study and understand mechanisms and behaviors connected to hydrate formation in different multiphase systems involving gas, oil and water. To further obtain insight into the different processes leading to hydrate deposition and blockage formation, a number of tests using a visual rocking cell have been performed in a gas-limited scenario with water, gas and liquid hydrocarbon mixtures. Various stages of hydrate formation were measured and observed under continuous mixing, as a factor of a number of variables (temperature, pressure, presence of thermodynamic inhibitors and anti-agglomerants). Phenomena such as deposition, sloughing, agglomeration and bedding were identified. In this work, a lower tendency to deposit on mineral oil wetted surfaces was observed, as compared to surfaces exposed to condensate or the gas phase. Nevertheless, hydrate deposition was also observed in the oil system, mainly at surfaces only exposed to the gas phase. A porosity analysis was performed for each experiment. Hydrate deposits with high porosity formed under high subcooling conditions, resulting in sloughing of the hydrate deposit due to the wetting and weight of the deposit. Another observed phenomenon was the phase separation during constant flow of the oil and water phases due to the incipient hydrate formation. This work presents some relationships between the phenomena observed (such as deposition, sloughing, agglomeration, bedding) and parameters, such as subcooling, porosity and type of liquid hydrocarbon in the system.*

Keywords*: Hydrates, Flow assurance, Multiphase flow*

1. INTRODUCTION

Gas hydrates are crystalline solids of water resembling ice, but with a crystalline structure of hydrogen bonded water molecules organized as regular polyhedrons with a water molecule in each of the vertices, hydrogen bonds as edges, and stabilized by gas molecules inside the polyhedrons. Light natural gas molecules like methane, ethane, propane, iso-butane, nitrogen, carbon dioxide, and hydrogen sulfide are among the molecules that may stabilize gas hydrates. While ice formation is a phenomenon mainly driven by temperature, gas hydrate stability depends on a combination of temperature, pressure and gas composition. Gas hydrates exist in nature as part of permafrost in arctic regions and in sediments beneath the ocean sea floor. Gas hydrates may also form at ambient temperatures above normal water freezing temperatures at high pressure in oil and gas transportation pipelines, and cause restrictions to flow due to their accumulation in the pipelines (Sloan and Koh, 2008).

The way gas hydrates form in pipelines depends on the phases present in the hydrocarbon system, the amount of each phase, the mixing among the phases, and the dispersion of phases. Hydrate will start forming at the water-hydrocarbon (oil and/or gas) interfaces. Cohesion due to capillary forces among hydrate-covered water droplets, and adhesion between these droplets and water wetted pipe wall, will result in hydrate agglomeration and deposition. These mechanisms influence the rheology, increase pressure drop, and can eventually cause formation of hydrate plugs (Sloan Sloan et al., 2008). Increased understanding of the conditions under which hydrate deposits form can contribute to the development of better hydrate management strategies. This paper presents an experimental study of hydrate formation specifically focused on deposition of hydrates on surfaces, with the combined observations of other mechanisms occurring during hydrate formation.

2. EXPERIMENTAL METHOD

2.1 Experimental setup

The experiments were performed at Colorado School of Mines in a high pressure cylindrical rocking cell with an internal diameter of 50.8 mm, internal length of 274 mm, and a total pressurized volume of 578 ml (Figure 1). It is installed horizontally and can be oscillated by a motor between positive and negative pipe inclinations, which results in mixing and gravity driven flow inside the rocking cell. The rocking cell is submerged in a water bath with transparent walls. The water is circulated through a chiller in order to maintain a constant temperature in the bath throughout an experiment. The upper surface in the rocking cell has a cooling chamber connected to a separate chiller that can be set to a different temperature than the bath temperature, to induce local formation of hydrate deposits in the upper part of the cell. The rocking cell is connected by a flexible hose to the gas filling and draining system, which consist of the gas supply line connected to a gas cylinder with the gas mixture used in the experiment, a safety pressure release valve, and the gas vent line. The pressure transducer measuring the total pressure of the system is installed where the flexible hose is connected to the gas filling and draining system. Temperatures are measured by thermocouples located in the following three positions in the rocking cell: at the upper pipe wall surface, in the gas phase close to the upper wall, and in the liquid phase close to the bottom. The development of flow characteristics, hydrate formation and deposition are visually monitored and documented by means of video recording through the windows (made of polycarbonate) measuring 145 × 34 mm on both side walls of the rocking cell.

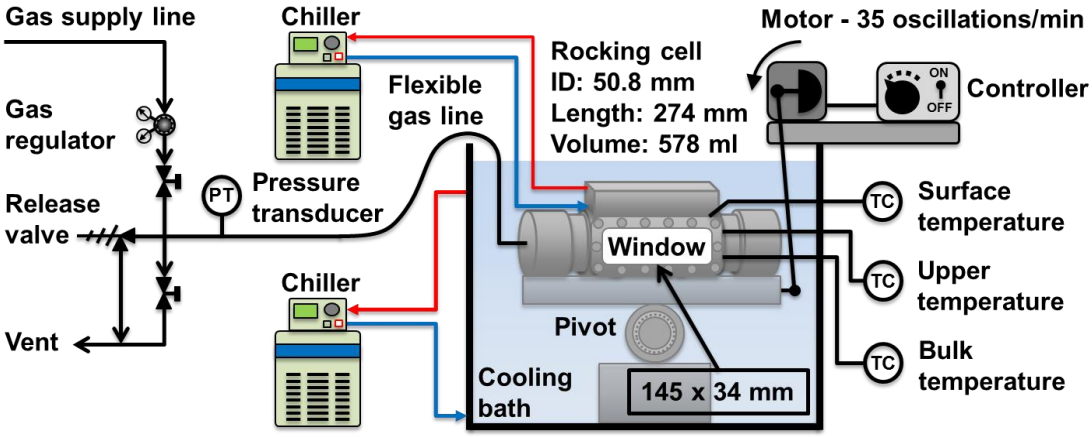

Figure 1. Schematic of the experimental setup for the rocking cell system for hydrate experiments.

2.2 Materials

The experiments were performed with a three-phase system of gas, liquid hydrocarbon, and aqueous phase. A gas mixture containing 74.7 mol% Methane and 25.3 mol% Ethane was used for all experiments. Mineral Oil 70T, Mineral Oil 200T (both purchased from STE Oil Company, Inc.), and a liquid sample from a gas condensate field were used as liquid hydrocarbon (Table 1). With respect to the aqueous phase, four systems based on tap water were used: pure water, a water solution of 3.5 weight percent (wt%) NaCl (Lab Grade), 6.6 wt% monoethylene glycol (MEG, ≥99%) in water and 0.5 wt% water solution of Arquad (a model anti-agglomerant purchased from Sigma-Aldrich Co.).

Table 1. Liquid hydrocarbon properties.

Property	Gas Condensate	Mineral Oil 70T	Mineral Oil 200T
Specific Gravity at 25 °C (kg/m^3)	660	825	856
Viscosity (cP) at 20 °C	0.264	21	47
Oil-Water Interfacial Tension (mN/m)	28	50	(not measured)
Average Molecular Weight	87	308	298

2.3 Experimental conditions

A total of 26 rocking cell experiments were performed with various filling compositions and cooling conditions, as listed in Table 2. Liquid loading is the total volume of liquids compared to the total volume. Water cut is the volume of water based on the total volume of liquids. The bath was cooled to temperatures between 1 and 9 °C in the experiments performed. In experiments with higher bath temperature than 1 °C, the upper wall was cooled to 1 °C. Cooling of the surrounding bath to a higher temperature resulted in lower sub-cooling, and a temperature gradient in the rocking cell

that favored hydrate deposition at the upper pipe wall. The pressure during an experiment decreased from about 39 bar before cooling to between 16 and 30 bar (depending on the cooling temperature) at hydrate equilibrium conditions at the end of the experiment. Consequently, the amount of water converted to hydrates also varies, depending on the pressure decrease due to hydrate formation during an experiment.

Table 2. Experiments performed with various combinations of fluids and experimental conditions.

Number of experiments	Liquid loading & water cut	Oil phase	Water phase	Bath temperature [°C]	Upper wall temperature [°C]	Water converted to hydrates [%]
6	70% LL & 60% WC	Mineral Oil 70T	Fresh water	1 – 9	1 or off	5.1 – 12.2
2	70% LL & 60% WC	Mineral Oil 200T	Fresh water	1 – 6	1 or off	7.5 – 8.0
5	70% LL & 60% WC	Gas Condensate	Fresh water	1 – 8	1 or off	8.3 – 21.2
3	70% LL & 60% WC	Mineral Oil 70T	3.5 wt% NaCl in water	1 – 6	1 or off	5.5 – 11.8
2	70% LL & 60% WC	Gas Condensate	3.5 wt% NaCl in water	1 – 6	1 or off	9.9 – 21.5
2	70% LL & 60% WC	Mineral Oil 70T	6.6 wt% MEG in water	1	off	11.5 – 15.7[1]
2	70% LL & 60% WC	Gas Condensate	6.6 wt% MEG in water	1	off	19.3 – 23.3[2]
2	70% LL & 60% WC	Mineral Oil 70T	0.5 wt% Arquad in water	1 – 6	1 or off	8.0 – 13.5
1	57% LL & 30 % WC	Mineral Oil 70T	0.5 wt% Arquad in water	1	off	52.4
1	59% LL & 30 % WC	Gas Condensate	0.5 wt% Arquad in water	1	off	76.4

[1]The first experiment was performed at 35.9 barg and 12.3 °C as initial conditions, after hydrates had first been formed at temperatures below 0 °C and dissociated. The second experiment was performed at 45.5 barg and 20.1 °C as initial conditions.
[2]The experiments were performed at 36.8 barg and 14.9 °C, and 39.6 barg and 15.2 °C, respectively, as initial conditions after hydrates had been first formed at temperatures below 0 °C and dissociated.

2.4 Experimental procedure

After a thorough cleaning procedure, the water, liquid hydrocarbon and additives (when required) were added by weight under atmospheric conditions; the flexible gas line and hoses to the chiller controlling the upper wall temperature were connected, and the rocking cell was placed in the temperature controlled bath. The rocking cell was then pressurized with gas to 38 barg at 20 °C and oscillated for about one hour at constant temperature, in order to saturate the liquid hydrocarbon phase with the gas mixture. The set point temperature of the chillers controlling the bath and upper pipe wall temperatures were changed from 20 °C to the experimental temperatures for a given experiment, and kept at these temperatures throughout the length of the experiment. The oscillation rate of the rocking cell was set to a constant value of 35 oscillations per minute throughout the entire experiment. After an experiment was stopped, the system was heated again to 20 °C. When the planned experiments for a given composition were completed, the system was slowly depressurized to atmospheric conditions. The flexible gas line and hoses to the chiller were disconnected, and the liquids of the rocking cell were drained into liquid waste disposal containers.

2.5 Analysis of experiments

Both quantitative and qualitative results are extracted for the experiments performed. The rocking cell is a closed system in which the exchange of components between phases and change of volumes of the phases are restricted to the conditions that both total volume and total amount of each component are constant in the system. The amount of hydrates formed and the hydrate equilibrium conditions in each experiment could therefore be calculated from the pressure and temperature data measured during the experiments, amount and composition of filled components (gas, the hydrocarbon liquid and the water phase), and total volume of the system. The calculations were performed with Multiflash® (KBC, 2014) using a Cubic-Plus-Association (CPA) equation of state. The volume of the hydrate deposits at the upper surface and bedded hydrates in the bulk was estimated based on images captured from the video recordings

and known dimensions of the cell and cell windows. This rough volume estimate and the calculated amount of hydrates formed were used to estimate the porosity of hydrates. The video recordings from the experiments also contributed with visual information, which in these cases was very insightful to understand the mechanisms of hydrate formation, deposition and accumulation during the experiments.

3. EXPERIMENTAL RESULTS AND DISCUSSION

3.1 Mineral oil systems

The experiment with gas mixture, 70% liquid loading, Mineral Oil 70T as oil phase, 60% water cut, cooling bath at 4 °C, and upper wall temperature at 1 °C, is used as an example presenting mechanisms for hydrate formation in the experiments with mineral oil and fresh water. Figure 2 shows the temperature and pressure traces, as well as hydrate equilibrium temperature, subcooling, and the amount of total water consumed to form hydrates (calculated based on the amount of gas consumed – pressure drop). The vertical dash lines A to G in the plot refers to specific key mechanistic events observed related to hydrate formation during the experiment. Before hydrate formation onset (Figure 2-A), the mineral oil and water phases were completely mixed in a shear-stabilized dispersion (see Figure 3-A). At the time of hydrate formation onset, the blue dyed oil and yellow dyed water phases separated within minutes before any significant amount of hydrates had formed or was observed, as shown in Figure 3-B, which is captured 4 minutes after the hydrate formation onset. Between 5 and 10 minutes after onset (Figure 2-B) hydrate deposits started appearing at the upper surface of the cell. The hydrates did not appear to deposit on the cell surface exposed to the liquid phase. Hydrates also started forming as particles in the water phase, which gradually transformed to a hydrate slurry with large agglomerates of hydrates about 30 minutes after hydrate formation onset (Figure 2-C).

About 52 minutes after hydrates started forming (Figure 2-D) some of the hydrates slough off the surface, as shown in Figure 3-C and 3-D. At this time, all the free liquid water was absorbed in the hydrate deposit or the bedded hydrate agglomerates in the lower part of the cell. Growth of highly porous hydrates and sloughing occurred repeatedly until 3 hours after hydrate formation onset in this particular experiment. The bedding of hydrates in the lower part started breaking up and flowing together with a free liquid phase between 5 and 7 hours after hydrate formation onset (Figure 2-E and F), and the volume of the deposit starts decreasing due to annealing or formation of hydrates with lower porosity. The pressure and temperature reached equilibrium conditions 10 hours after hydrate formation started (Figure 2-G) and there were just minor fluctuations in the measurements after this time. Less than 12% of water available was converted to hydrates in this experiment, because the hydrate formation was limited by the available gas before the pressure reached equilibrium conditions.

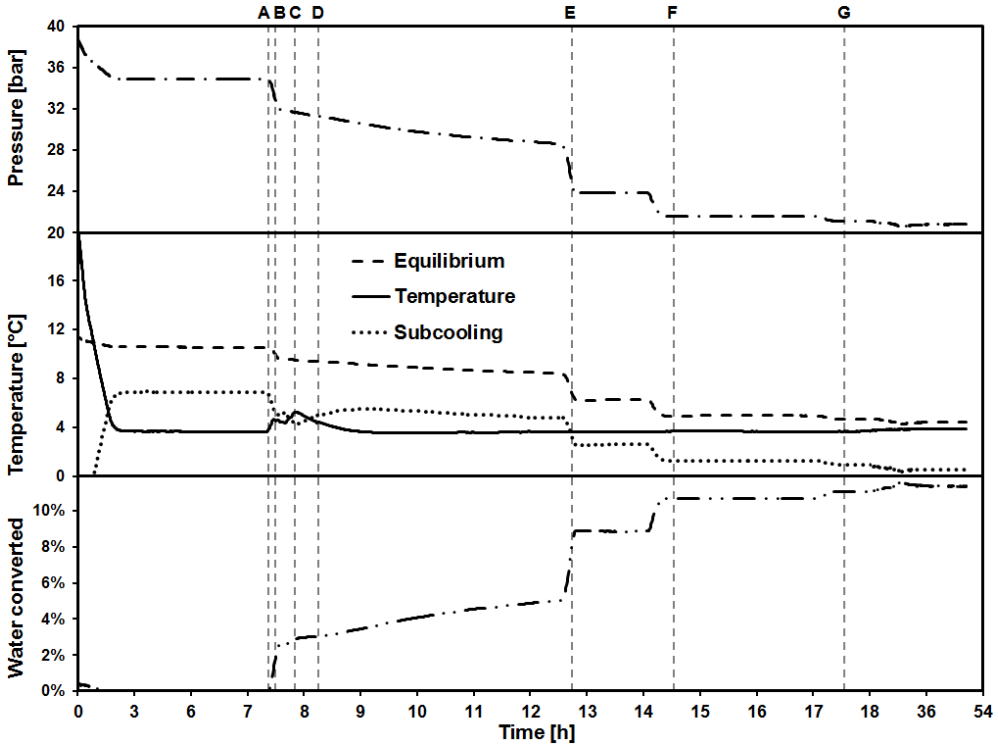

Figure 2. Measured and calculated results from a rocking cell experiment with observations during the experiment. The vertical dash lines A to G in the plot refers to specific key mechanistic events observed related to hydrate formation during the experiment. Time axis is compressed before 6 h and after 18 h for clarity.

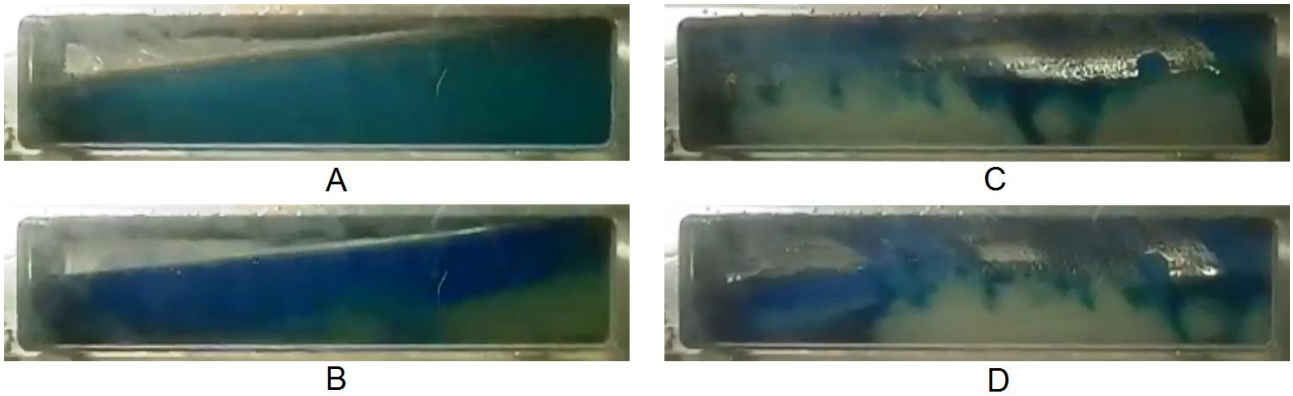

Figure 3. Phase separation: (A) Dispersion before hydrate formation started. (B) Phase separated oil (blue) and water (yellow) 4 minutes after hydrate formation onset. Sloughing and bedding: (C) Hydrates attached to the surface in the upper left part of the window, (D) sloughed off the wall and entered the oil phase with bedded hydrates.

3.2 Gas condensate systems

The experiments with the methane + ethane gas mixture, condensate and fresh water resulted in similar pressure decrease due to hydrate formation as the experiments with mineral oil. However, more gas dissolves in condensate than mineral oil, which resulted in more gas and water converting to hydrates before the pressure decreased to the hydrate equilibrium at the experimental temperature compared to equivalent experiments with mineral oil. About 20% of the water was converted to hydrates when the experiment was stopped 96 hours after hydrate formation onset.

The mechanisms for hydrate formation and deposition in the experiments with condensate showed both similar and different characteristics to those observed in the experiments with mineral oil. In the experiments with condensate and fresh water, the liquid phases were partly dispersed before hydrate formation. An oil in water dispersion with low content of condensate formed in the water phase before hydrate formation due to the flow (Figure 4-A). This dispersion phase separated within five seconds upon hydrate formation onset. About five seconds after the phase separation, hydrate particles started appearing at the interface between the condensate and water phases. Thirty seconds after hydrate formation onset a thick layer of hydrate particles had formed at the interface, as shown in Figure 4-B. As more water was converted to hydrates, the water phase transformed to a hydrate slurry with increasing viscosity (Figure 4-C, captured two minutes after hydrate formation onset). The increased hydrate content resulted in bedding and no liquid flow. The bedding of hydrate particles ultimately formed a solid deposit of hydrates when more of the water in-between the hydrate particles were converted to hydrates. There was no visual difference observed in the video between one hour after hydrates started forming (Figure 4-D) and the end of the experiment. The images are captured from video recordings of the experiment where the whole rocking cell was cooled to 1 °C.

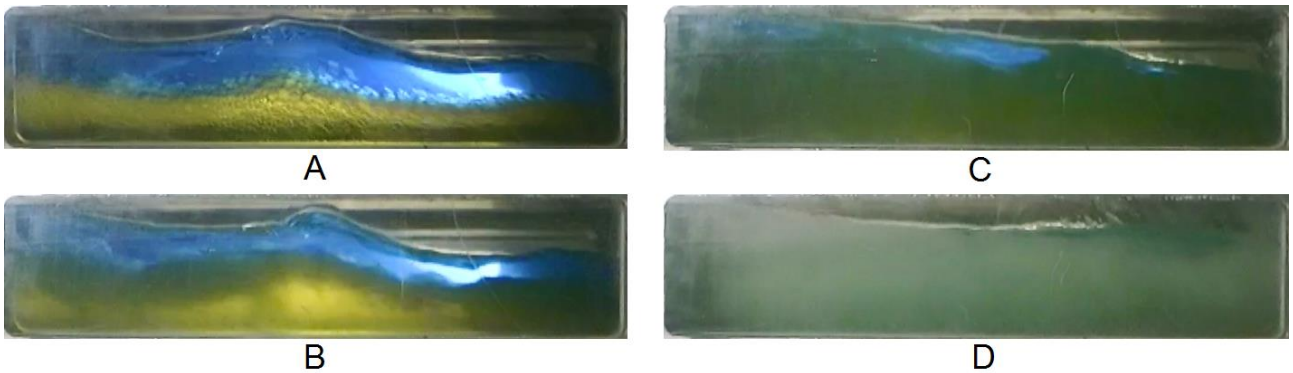

Figure 4. Before hydrate formation: (A) Condensate (blue) and water in oil dispersion (yellow). Various stages of the hydrate formation: (B) Hydrates can be seen as particles at the water/condensate interface 30 seconds after hydrate onset, (C) dispersion of hydrate particles in water, and (D) a solid hydrate deposit.

In the experiments with a temperature gradient between the upper wall and the bath, hydrates started depositing mainly at the upper wall, but there were also some deposits in the rest of the rocking cell. Similar to the mineral oil experiments, sloughing and agglomerates of hydrates in the liquid phase were also observed in these experiments. For the experiment with condensate and fresh water with cooling of the bath to 8 °C and upper cell surface to 1 °C, sloughing continued throughout the entire experiment.

3.3 Phase separation of dispersion due to hydrate formation

One interesting observation from the experiments performed is the phase separation or change in the dispersion state of water in the oil phase at the onset of hydrate formation shortly before hydrates were detected visually and by pressure drop. As shown in Figure 5, the mechanism observed can be divided into three steps: i) Entrainment: phases are dispersed due to shear forces from the flow in the rocking cell. The oils tested are non-emulsifying, which imply a low content of surface active components. The dispersion will therefore quickly phase separate if the flow and mixing in the cell is stopped. ii) Initial Formation: Hydrates can form at all interfaces between water and hydrocarbon containing hydrate forming components. iii) Phase Separation: liquid hydrocarbon and water phases quickly phase separate shortly after hydrate formation onset with a macroscopically undetectable amount of hydrates. Dispersion of the oil and water phases before hydrate formation could be observed in all the systems studied, but it had different visual appearance in the various systems. The Mineral Oil 70T and fresh water were fully dispersed before hydrate formation, while condensate and fresh water formed a partly dispersed system of a separate condensate phase and water in oil dispersion with a very low oil content resembling a foam structure. This foam structure, which broke down within seconds when hydrates started forming, seemed to be much more "fragile" to the influence of hydrates than the fully dispersed water in mineral oil system, in which the phases gradually separated in the first 4 minutes after hydrates formation onset.

The phase separation in all the systems tested indicates that there is a connection between the present of hydrates in a system and dispersion of the phases. The cause of the phase separation mechanism is yet not fully understood, but it is likely related to the instantaneous change in the fluid viscosity, interfacial tension, and gas concentration when the gas in the oil phase is consumed due to the initial hydrate. An alternative explanation is that the hydrate particles forming at the oil/water interface might destabilize dispersions due to the hydrate surface energy properties, similar to the theory that demonstrates how particles with certain surface energy properties may stabilize emulsions and foams (Aveyard et al., 2003; Hunter et al., 2007).

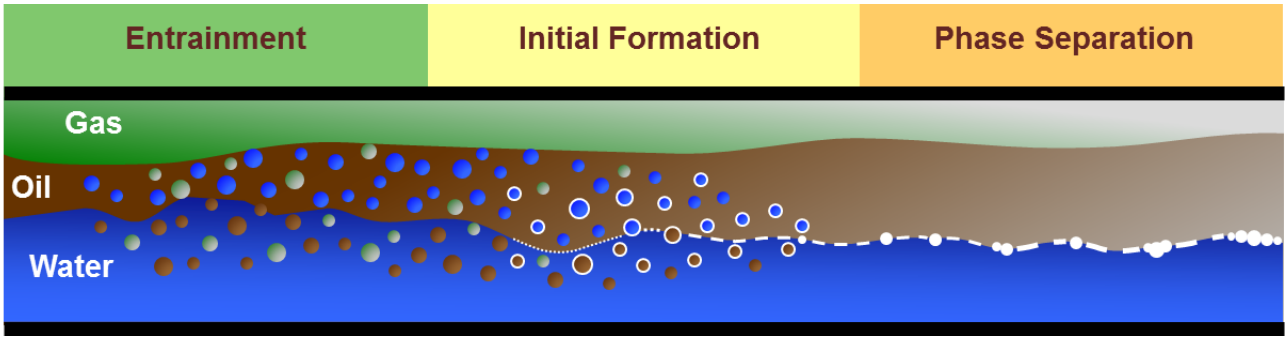

Figure 5. Steps leading to phase separation: Entrainment: phases are dispersed before hydrate formation due to shear forces from the flow; Initial Formation: hydrates form at all hydrocarbon-water surfaces; and Phase Separation: hydrate formation causes the liquid hydrocarbon and water phases to separate in flowing conditions.

3.4 Deposition, sloughing and porosity

Deposition of hydrates was the principle topic of this experimental study. Video recordings from the experiments show that hydrates deposited at all surfaces in experiments with condensate, while hydrates had a higher tendency to deposit at surfaces that were not wetted by the oil phase in the experiments with mineral oil. Sloughing was observed in a majority of the experiments with fresh water and with mineral oil and condensate as oil phase, and also in some of the experiments with NaCl or MEG in the water phase. The observations from the various experiments indicate that the volume and porosity of the formed deposits depends on the subcooling of the system. High volume and low amount of water converted to hydrates signify that the porosity of the deposits was high and the solid content ensuring structural stability of the deposits was low. The highly porous deposits enclosed a large quantity of liquid water, and the weight and low solid content caused the sloughing events. The deposits of lower volume and higher solid content were structurally more stable and sloughing did not occur when these deposits formed.

Based on the observations from the experiments, the hydrate formation mechanisms related to hydrate deposition can be divided into three steps, as indicated in Figure 6. The first step is the formation of deposits of high volume and porosity at the upper wall surface of the cell and some hydrate formation in the bulk liquid phases for conditions of high subcooling ("Deposition" in Figure 6). This is followed by sloughing of the hydrate deposit ("Sloughing", Figure 6); the large chunks of hydrate break off the deposit at the wall and flow with the liquid. Some experiments, in which the upper wall surface was cooled to a lower temperature than the surrounding bath, demonstrated repeating formation of deposits of high volume and sloughing, with the sloughed hydrates broken down in the liquid phase (return to "Deposition" in Figure 6). In some of the experiments with low temperature gradient in the cell, hydrates of much lower volume formed at the upper wall surface after the calculated hydrate equilibrium temperature had decreased and stabilized at a value close to the measured cell temperature due to the pressure decrease ("Annealing" in Figure 6).

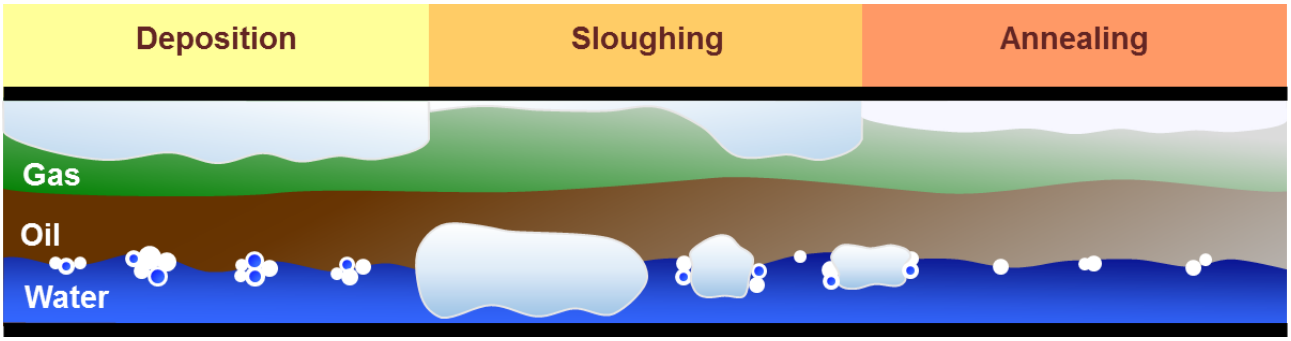

Figure 6. Illustration of hydrate formation and accumulation observed in the experiments. Initial formation of hydrate deposits of high volume and porosity at high subcooling. Sloughing, and Annealing or formation of deposits with lower volume and porosity at conditions close to hydrate equilibrium.

3.5 Hydrate particle growth, agglomeration and bedding

In addition to deposition at the cell surfaces, hydrate formation in the bulk liquid phase and bedding were observed in the majority of the experiments. This starts as hydrate growth at all hydrocarbon-water interfaces as illustrated in the first stage in Figure 7. As the hydrate content increases, the apparent liquid viscosity increases. In some of the experiments the hydrates were dispersed in the water phase, while the oil phase appeared transparent without any water or dispersed hydrates. These dispersed hydrate particles can agglomerate, as shown in the second stage in Figure 7. As the agglomerates of hydrates grow larger, all free water becomes occluded in the agglomerates, which may not move along with the oil flow in the cell. This can be considered the bedding, the final stage in Figure 7. Hydrate agglomeration was the dominant hydrate formation mechanism in the experiments with gas mixture, mineral oil and water with MEG, which lead to bedding and blockage of the entire cross section of the rocking cell with agglomerated hydrates; this outcome would have been characterized as a hydrate blockage had it happened in a pipeline. These results indicate that an increased level of agglomeration at low concentrations of MEG could increase the risk of plugging of a pipeline where the injection amount of MEG causes the system to be under-inhibited.

The experiment with gas mixture, condensate and fresh water with cooling of the rocking cell to 1 °C demonstrated a slightly different bedding mechanism. After an initial growth of hydrate particles at the condensate/water interface, all of the condensate and water with hydrates was transformed to a dispersion with increasing hydrate content and increasing viscosity. This dispersion eventually stopped flowing because of the high viscosity, which could be defined as bedding of the hydrate particles. Further hydrate growth from unconverted water in-between the hydrate particles resulted in formation of a continuous hydrate deposit. The experiment with gas mixture, mineral oil and 30% water cut with 0.5% Arquad showed that the AA prevented the agglomeration of hydrate particles. The early stages of that particular experiment revealed some tendency of partly phase-separation and agglomeration (second stage in Figure 20). The conditions then returned to hydrate particle growth (first stage in Figure 20), and a transportable hydrate slurry was formed. These results demonstrate that use of AA as a flow assurance strategy might be a good option for fields where other approaches are less economically viable.

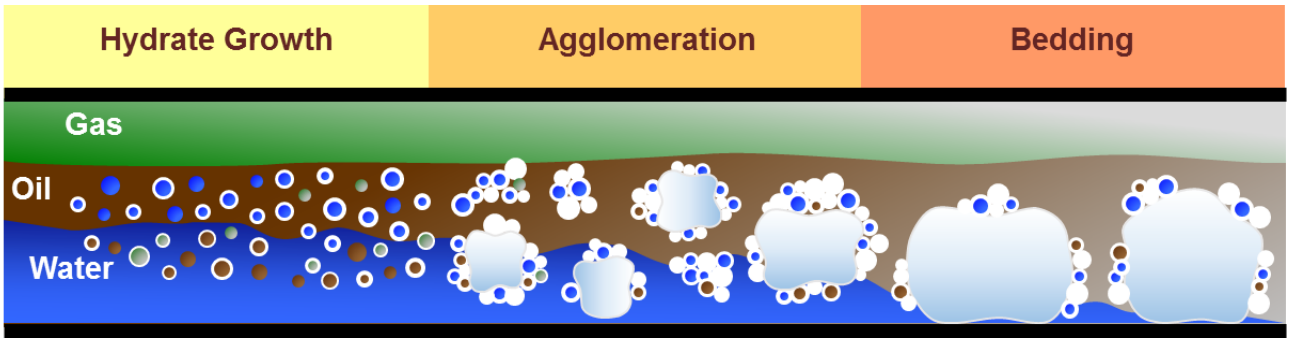

Figure 7. Steps in formation, agglomeration, and accumulation of hydrates as observed in the rocking cell experiments for predominant bulk hydrate.

3.6 Hydrate formation in non-emulsifying systems

The mechanisms and behaviors connected to hydrate formation were observed to various degrees depending on the fluid system and conditions of the experiments. The experiments show that rather than exclusively considering deposition as hydrate formation mechanism for some systems and exclusively agglomeration in other systems, it would

be more accurate to consider a combination of various mechanisms for the different systems with agglomeration as the most dominant mechanism in certain systems and deposition-related mechanisms in others. Based on the observations and measurements in this study, a revised conceptual model for hydrate formation in non-emulsifying systems has been developed, as shown in Figure 8, which combines all the observed hydrate formation mechanisms. The first stage is entrainment of the phases due to the shear imposed by the flow. The second stage is phase separation of the shear-stabilized dispersion at the time of hydrate onset before any significant amount of hydrates is formed or macroscopically detected. In the third stage, hydrates grow as particles dispersed in the liquid phases and as deposits on the pipe wall. The fourth stage includes agglomeration of hydrate particles, sloughing of hydrates from the pipe wall and bedding of hydrates that can no longer be transported with the liquid flow in the pipe. These mechanisms will eventually lead to build up of hydrates and plugging of the pipeline, which is the last stage.

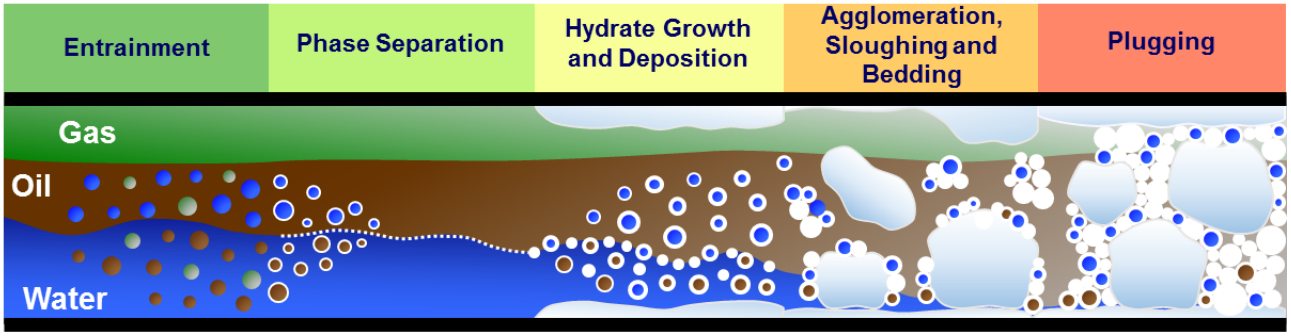

Figure 8. Revised conceptual model for hydrate formation and accumulation in shear stabilized dispersion (non-emulsifying oil).

4. FUTURE WORK

Future work will include investigating the suitability of generate results to formulate models and correlations for deposition tendency and thickness as a function of the variables used in the tests.

5. CONCLUSIONS

Hydrate formation, deposition, and accumulation mechanisms in various hydrocarbon systems have been observed and measured experimentally in a rocking cell with visual capabilities. The experiments demonstrated combination of various mechanisms with agglomeration as the most dominant in certain systems and deposition in others. Some phase separation of the dispersed phases was detected at the onset of hydrate formation in all the tested hydrocarbon systems. The cause of this instantaneous and brief phase separation is not yet fully understood. Hydrate deposits with high porosity and sloughing were observed in the experiments when the subcooling was high and when there was a high temperature gradient in the cell, while deposits with lower porosity formed when the subcooling and temperature gradient was low. Hydrates deposited mainly at the upper cell surface, which was not directly exposed to liquid flow in the experiments with mineral oil, whereas hydrates deposited at all surfaces in the experiments with condensate. Under-inhibited systems can under certain conditions have an increased risk of hydrate agglomeration compared to non-inhibited systems. Anti-agglomerants promote formation of transportable hydrate slurry, but transient agglomeration of hydrates could be observed at low concentration of AA.

6. ACKNOWLEDGEMENTS

This research was funded by Repsol Sinopec Brasil supported by the R&D Levy of the ANP – The National Agency of Petroleum, Natural Gas and Biofuels, Brazil.

7. REFERENCES

Aveyard, R., Binks, B.P. and J. H. Clint., 2003. “Emulsions stabilised solely by colloidal particles”. Advances in Colloid and Interface Science, Vol. 100-102, pp. 503-546.

Hunter, T.N., Pugh, R. J., Franks, G. V. and Jameson, G. J., 2008. “The role of particles in stabilising foams and emulsions”. Advances in Colloid and Interface Science, Vol. 137, No. 2, pp. 57-81.

KBC, 2014. Multiflash 4.4, Infochem/KBC Advanced Technologies plc.

Sloan, E.D. and Koh C.A., 2008. Clathrate Hydrates of Natural Gases, third ed. CRC Press, Taylor & Francis Group. Boca Raton, FL.

Sloan, E.D., Koh, C.A. and Sum, A.K., 2011. Natural Gas Hydrates in Flow Assurance. Elsevier Inc., New York